ACS APPLIED MATERIALS & INTERFACES

Research Article

www.acsami.org

Fabrication of Microscale Hydrogels with Tailored Microstructures based on Liquid Bridge Phenomenon

Lin Wang,[†,‡,§] Mushu Qiu,[†,‡,§] Qingzhen Yang,[†,‡] Yuhui Li,[†,‡] Guoyou Huang,[†,‡] Min Lin,[†,‡] Tian Jian Lu,[‡] and Feng Xu*[,†,‡]

[†]The Key Laboratory of Biomedical Information Engineering of Ministry of Education, School of Life Science and Technology, Xi'an Jiaotong University, Xi'an 710049, China

[‡]Bioinspired Engineering and Biomechanics Center (BEBC), Xi'an Jiaotong University, Xi'an 710049, China

Supporting Information

ABSTRACT: Microscale hydrogels (microgels) find widespread applications in various fields, such as drug delivery, tissue engineering, and biosensing. The shape of the microgels is a critical parameter that can significantly influence their function in these applications. Although various methods have been developed (e.g., micromolding, photolithography, microfluidics, and mechanical deformation method), it is still technically challenging to fabricate microgels with tailored microstructures. In this study, we have developed a simple and versatile method for preparing microgels by stretching hydrogel precursor droplets between two substrates to form a liquid bridge. Microgels with tailored microstructures (e.g., barrel-like, dumbbell-like, or funnel-like shapes) have been achieved through adjusting the distance between and the hydrophobicity of the two substrates. The developed method holds great potential to impact multiple fields, such as drug delivery, tissue engineering, and biosensing.

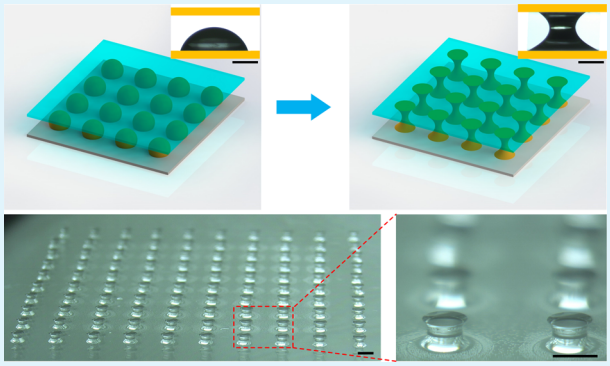

KEYWORDS: *microscale hydrogel, liquid bridge, tailored microstructure, tissue regeneration, microgel assembly*

1. INTRODUCTION

Microscale hydrogels (microgels), considered as three-dimensional (3D), water swollen, soft polymer materials at microscale and with tunable chemical and physical properties, find widespread applications in biomedical fields, for example, as carrier in drug delivery systems,[1] building blocks in tissue regeneration,[2] and sensing units in biosensing.[3] The shape of the microgels is considered as a critical parameter that can significantly influence their function in such applications.[4] For instance, cell-laden microgels with various shapes have been developed to mimic the repeating functional units in human body and to be assembled into large and complex cellular constructs for remodeling tissues in vitro.[5−10] Additionally, disc shaped microgels as drug carriers have been found to give an enhanced targeting efficiency compared to microgels with spherical shape.[11] Therefore, it is desirable and necessary to fabricate microgels with tailored microstructures to achieve specific functions.[12]

Various methods have been developed to fabricate microgels with different shapes (e.g., cube, rod, and disk), including micromolding,[13,14] microfluidics,[15,16] photolithography,[17,18] and mechanical deformation method.[19] Although these methods have several advantages including high throughput and controllability of microgel shape, they are associated with several limitations. For instance, micromolding method involves the potential issue of mechanical deformation and damage during the lift-off process, which may lead to nonuniformity of microstructures. Microfluidics needs precisely designed microchannels and complex devices, which may limit its wide access. Photolithography method is widely used due to its advantages, such as simple, programmable pattern, and high throughput. Doyle et al. fabricated nonspherical hydrogel and barcoded hydrogel by integrating photolithography and microfluidics.[20−23] However, the thickness and materials of the fabricated hydrogel is limited, and its microstructure is limited due to the deflection of the light.[24] In addition, microgels fabricated from these approaches are mostly limited to cylindrical objects or need to be immersed in oil involving potential issue of biocompatibility. For mechanical deformation method, spherical particles made of temperature-sensitive polymer (polystyrene) are encapsulated in poly(vinyl alcohol) by suspending particles in polymer solution, and different shaped microparticles (e.g., sphere, elliptical disk, and rod) can be obtained by melting the particle and subsequently stretching the poly(vinyl alcohol) polymer.[19] In another study, microgels with different shapes (e.g., barrel-like, dumbbell-like) were also

Received: January 8, 2015
Accepted: March 2, 2015
Published: March 2, 2015

DOI: 10.1021/acsami.5b00081
ACS Appl. Mater. Interfaces 2015, 7, 11134−11140

fabricated by simultaneously compressing and heating spherical particles of temperature-sensitive polymer between two plates.[25] However, the mechanical deformation method is limited to temperature-sensitive materials. Besides, most of such materials tested are not biodegradable. Therefore, there is still an unmet need for a simple and versatile method to fabricate microgels with tailored microstructures that are compatible with different hydrogels.

The formation of a liquid bridge between two solid surfaces is a common phenomenon observed in nature. For instance, many insects (e.g., beetles and blowflies) form micro liquid bridges between their attachment pads and surfaces with secretory liquid to enhance adhesion to the surface.[26−29] Such phenomenon has been widely used in industry (e.g., for transferring ink in the printing industry and dispensing glue in the packaging industry[30−33]) and recently utilized for generating drop-on-demand to encapsulate a single cell without the need for complex control or external equipment.[34] It has been known that the shape of the liquid bridge can be tuned by controlling the contact angles and distances between two surfaces.[32,35] This inspires us to apply liquid bridge for microgel fabrication, which, however, has not been explored yet.

In this study, we report a simple and facile method to fabricate microscale hydrogels with tailored microstructures based on liquid bridge phenomenon. This method involves placing a droplet of hydrogel precursor solution on a substrate, forming a liquid bridge with another substrate, and then cross-linking the liquid bridge to generate microgels. Different shaped hydrogel units (e.g., barrel-like, dumbbell-like, or funnel-like) were successfully fabricated in a high-throughput manner. The applicability of such a method to temperature-, photo-, and chemical-sensitive hydrogels was verified. The developed method holds great potential in drug delivery, tissue regeneration, and biosensing applications.

2. EXPERIMENTAL SECTION

2.1. Materials. Gelatin, polyethylene glycol (PEG), gelatin-methyl acrylate (Gel-MA) and polyacrylamide (PAAm) hydrogels were used, representing temperature-, photo-, and chemical-sensitive hydrogels, respectively. Gelatin was purchased from Sigma-Aldrich. PEG-DMA 1000 was obtained from Polysciences, Inc. Gel-MA was synthesized as reported before.[36] Photoinitiator, (2-hydroxy-2-methylpropiophenone), was received from TCI (Shanghai). Acrylamide, *N*,*N*′-methylenebis(acrylamide) (MBA), and *N*,*N*,*N*′,*N*′-tetramethylethylenediamine (TEMED) were obtained from MP Biomedicals. Ammonium persulfate (APS) was purchased from Spectrum Chemical. Super hydrophobic glass cleaner (ZXL-CSS) was obtained from ZIXILAI Environmental Protection Technology Co., Ltd. Poly(methyl methacrylate) (PMMA) was purchased from Evonik Industries.

2.2. Preparation of Substrates and Hydrogel Precursors. Three different kinds of surface were used in this experiment (i.e., carry sheet glass, PMMA, and hydrophobic glass). Glass and PMMA were used directly. Hydrophobic glass was prepared by painting the super hydrophobic glass cleaner on the glass surface with a high-density sponge. Then, the cleaner-treated glass was dried at room temperature. We measured the contact angle of each surface with water, and they are ∼11° on glass, ∼81° on PMMA and ∼93° on hydrophobic glass, respectively. Obviously, the super hydrophobic glass cleaner greatly increased the contact angle, but it still did not reached the super hydrophobic range, which requires the contact angle to be larger than 150°. Different shapes of PMMA substrates were fabricated by cutting the PMMA with a laser cutting machine (Versa LASER 2.30 mini Desktop Laser Engraving Machine).

PEG precursor was prepared by dissolving PEG and the photoinitiator in water, with final concentration of 10−20 and 0.5 wt %, respectively. Gel-MA precursors were prepared by dissolving Gel-MA and the photoinitiator in water, with final concentrations of 5 and 0.3 wt %, respectively. PAAm precursor was prepared as follows. Acrylamide (16.6 wt %), APS (0.291 wt %) and MBA (0.0623 wt %) were dissolved in beakers with water. The solution was stirred until it turned transparent. Finally, we added the TEMED (catalyst), rapidly mixed the solution, and put it into use instantly. Gelatin precursor was prepared through dissolving the gelatin powder in water at 50 °C and the final concentration was 5 wt %.

2.3. Fabrication of Liquid Bridge and Microgels. To fabricate microgels, we first form liquid bridges. For this, we used a lift platform that consists of two parts: the lower side is a fixed stage, and the upper side is a movable arm with a joint that can adjust the moving direction of the arm (from vertically to horizontally). The arm can move by adjusting a knob, and the arm moves 240 μm when the knob rotates an entire circle. To form the liquid bridges, three steps are needed. First, paste a substrate on the upper side of the lift platform with double-sided adhesive tape. Next, loosen the joint, and move the arm until the substrate is just against the lower stage, which ensures that the two substrates are parallel in the following process. Fix the joint, put another substrate in the lower stage, and pipet a drop of hydrogel precursor on the substrate. Then, the liquid bridges form between the two substrates by moving the arm. Subsequently, adjust the knob to stretch or compress the liquid bridge at a low speed to get the intended shape. Finally, cross-link the hydrogel precursor in different ways (e.g., UV radiation for PEG (25 s at 100% power with OmniCure SERIES 2000), cooling for gelatin (at 16 °C), chemical catalyzing for PAAm).

2.4. Optical Imaging. An optical microscopy of ultradepth field produced by KEYENCE (VHX-600E) was used to image the fabricated microgels. Both the shape and size can be analyzed through the obtained photos. We also used the photos to calculate contact angles and the distance between two surfaces.

2.5. Mathematical Modeling. To get better understanding of liquid-bridge-based microgel formation, we also developed a mathematical model to investigate the liquid bridge numerically. A typical liquid bridge is illustrated in Scheme 1; a droplet of liquid is confined between two solid flat surfaces with a separation H. Due to the action of surface tension, the liquid would take an axisymmetric meniscus profile. The contact angle at the lower (upper) plate is represented by θ_1 (θ_2). At equilibrium, the profile of the liquid bridge is governed by the following equations:[30,35,36]

Scheme 1. Geometry and Coordinate System for the Liquid Bridge

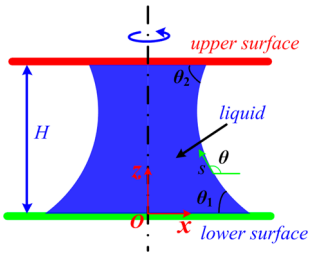

$$\begin{cases} \dfrac{dx}{ds} = \cos\theta \\ \dfrac{dz}{ds} = \sin\theta \\ \dfrac{d\theta}{ds} = \dfrac{\Delta P}{\gamma} - \dfrac{\rho g z}{\gamma} - \dfrac{\sin\theta}{x} \end{cases} \quad (1)$$

where θ is the angle between the tangential direction of liquid surface, and x axis as depicted in Scheme 1; ρ represents the density that the liquid bears and γ is the surface tension coefficient of liquid/air interface; Δp is the pressure difference between the inside and outside of the liquid, which is a constant because the liquid bridge is in

DOI: 10.1021/acsami.5b00081
ACS Appl. Mater. Interfaces 2015, 7, 11134−11140

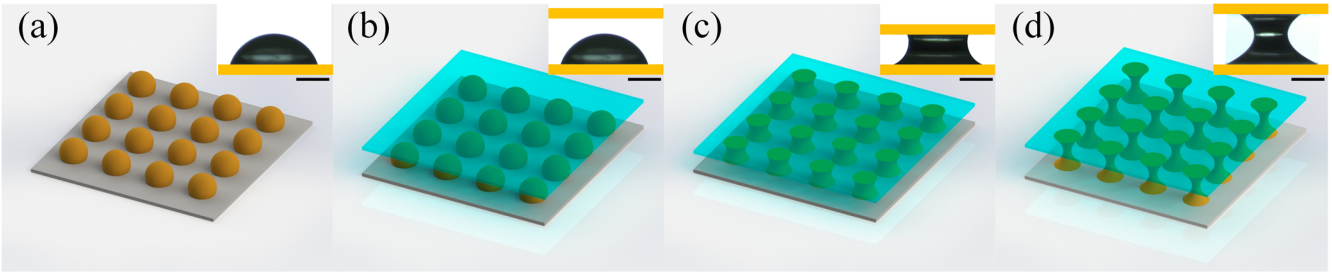

Figure 1. Schematic of microgel fabrication methods. (a–d) Schematic of fabrication method. The insets are images of products in different process (gelatin was used). All the substrates were PMMA. Scale bar: 500 μm.

equilibrium. Essentially, the first two equations describe geometry relations, and the third one is from the Young–Laplace equation,[37] indicating force balance at the interface. As pointed by some researchers, gravity is usually ignorable in the system if the scale is small.[35,36] In this study, however, the gravity term is still retained as we focus on general cases. For convenience, the first two equations are rewritten and then substituted into the third one. The governing equations can be recasted as

$$\frac{d^2x/dz^2}{[1 + (dx/dz)^2]^{3/2}} - \frac{1}{x\sqrt{1 + (dx/dz)^2}} + \frac{\Delta P}{\gamma} - \frac{\rho g z}{\gamma} = 0 \tag{2}$$

which is a nonlinear ordinary differential equation. By doing this, only one equation needs to be solved instead of three.

Boundary conditions at the two end points ($x = 0$ and $x = H$) are needed to solve the governing equation. One intuitionistic idea is to fix the contact angles at the upper and lower plate. However, due to the effect of hysteresis, contact angles are not necessarily constant but can change between advancing and receding values. According to Chen et al.,[35] two different types of boundary conditions may exist for liquid bridge problem. The first condition is that contact angle is specified (i.e., Neumann boundary condition), which, take the lower plate for instant, can be expressed as

$$\left.\frac{dx}{dz}\right|_{z=0} = -\cot\theta_1 \tag{3}$$

The other condition is that the contact line is pinned (i.e., Dirichlet boundary condition), thus the location of contact line is prescribed as

$$x|_{z=0} = x_1 \tag{4}$$

Similarly, the boundary condition at the upper plate is,

$$\left.\frac{dx}{dz}\right|_{z=H} = \cot\theta_2 \tag{5}$$

or

$$x|_{z=H} = x_2 \tag{6}$$

If the contact angles are between advancing and receding values, the contact line is pinned. However, if the contact radius changes, the contact angle would remain fixed, either advancing or receding values. An extra equation is needed because, in eq 2, Δp is still unknown, and its value is determined by a constraint equation,

$$\int_0^H \pi x^2 dz = V_0 \tag{7}$$

where V_0 refers to the initial volume of the liquid bridge. Physically, eq 7 indicated that the volume is conserved.

To enable the numerical solution, the Garlerkin finite element method[38] was employed to solve eq 2 with the associated boundary conditions. The details of the numerical method has been described elsewhere,[39] and only a brief introduction is given here. The entire segment is discretized into n elements, where n is chosen as 30 in our case. For each element, the governing equation is multiplied by the weighting function and, one has the weak form formulation after integrating by parts. Applying the above procedure to all the elements, a set of algebraic equations are obtained and can be assembled into one matrix afterward. The discrete points on the interface (x_i, z_i) can be obtained by solving the matrix. For free surface calculations as described above, a quadratic polynomial approximation yields more accurate results.[38]

2.6. Cell Encapsulation. NIH 3T3 mouse fibroblasts were used for cell encapsulation and cell viability tests. The cells were maintained in Dulbecco's modified Eagle's medium (DMEM) supplemented with 10% FBS and 1% penicillin streptomycin in a 95% humidity and 5% CO_2 incubator at 37 °C. When the 3T3 cells were encapsulated in the precursor solution, the cells were trypsinized and resuspended in the prepolymer solution at a concentration of 1×10^7 cells/ml. Cell viability was characterized by incubating cells with Live/Dead dyes (0.25 μL of calcein AM and 1 μL of ethidium homodimer-1 in 300 μL of Dulbecco's phosphate-buffered saline (DPBS)) for 20 min, and then imaged using fluorescent microscope. Number of live and dead cells were quantified by using software Image Pro Plus.

2.7. Assembly of Microgels. The microgels with dumbbell-like shape were prepared following the method described above (20 wt % PEG and glass were used), and the rod-shaped microgels were fabricated following a method reported before (20 wt % PEG was used).[40] The microgels were assembled by using the thermodynamic properties of multiphase liquid–liquid systems as reported by Du et al.[2] The microgel assembly can be controlled by the forces involved in minimizing the surface free energy between the oil/water interface.

3. RESULTS AND DISCUSSION

To obtain the liquid bridge of polymer precursor, we developed a simple and facile method, which is shown in Figure 1. At first, a drop of hydrogel precursor was dropped on the lower substrate (Figure 1a). Then, another substrate was placed in the upper side of the lift platform (Figure 1b). The separation between two kinds of substrate can be regulated by adjusting the lift platform, and finally a liquid bridge between the two substrates was formed (Figure 1c). The intended shape of the liquid can be obtained by stretching or compressing the liquid bridge between two solid surfaces (Figure 1d). The shapes of the liquid bridges were mainly controlled by both the distance between the two substrates (H) and the wetting behavior of liquid on the substrate, suggesting that various shapes of liquid bridge can be easily fabricated. The liquid bridge was subsequently cross-linked, and the anisotropic microgel was obtained. Images of real products in different processes were shown in the inset of each schematic diagram.

To explore the minimum and maximum sizes of the microgel, we did a series of experiments. To obtain various sizes of fabricated liquid bridge microgels, we controlled the volume of the hydrogel precursor by using microliter syringes. Different sizes of microgels were obtained, and the results are showed in Figure 2a. The volume of the hydrogel precursor was

DOI: 10.1021/acsami.5b00081
ACS Appl. Mater. Interfaces 2015, 7, 11134–11140

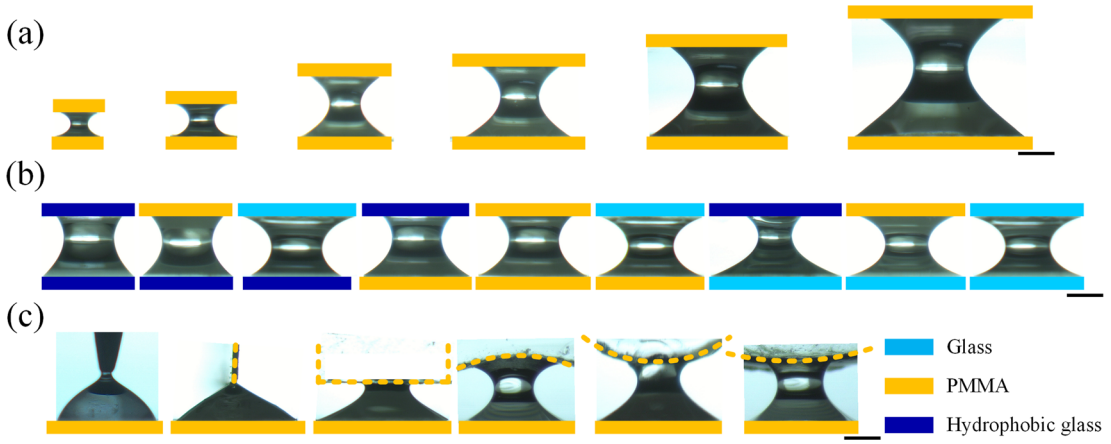

Figure 2. (a) Microgels fabricated with droplet volumes of (left to right) 0.05, 0.1, 0.3, 0.5, 1, and 2 μL. (b) Microgels fabricated with different surfaces; (c) microgels fabricated with different shapes of the substrates (the substrates were a needle, a slice of PMMA (front and side views), and cambered surface with different radius of curvature, respectively). All the material used for experiment was gelatin. Scale bar: 500 μm.

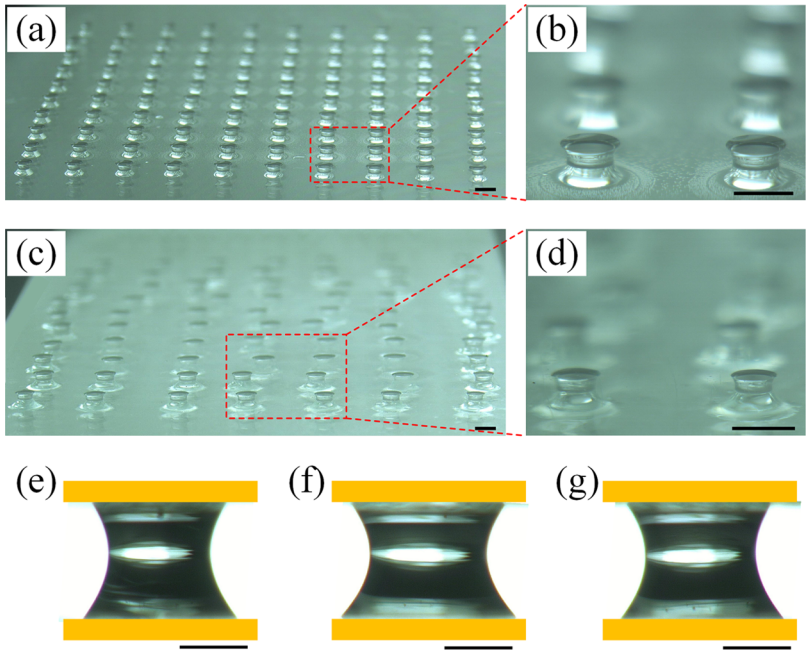

Figure 3. (a) Microgel array fabricated with PMMA on both sides; (b) magnified image of panel a; (c) array fabricated with hydrophobic glass on the upper side and glass on the lower side, 20% PEG was used; (d) magnified image of panel c. Scale bar: 1000 μm. Fabrication of multiple kinds of microgels using temperature-sensitive hydrogel (gelatin), photosensitive hydrogel (PEG), and chemical cross-linked hydrogel (PAAm); (e) temperature-sensitive hydrogels (gelatin); (f) photosensitive hydrogel (10 wt % PEG); (g) chemical cross-linked hydrogel (PAAm). The substrates were PMMA. Scale bar: 500 μm.

0.05, 0.1, 0.3, 0.5, 1, 2 μL respectively, and the size of the microgels were from 400 μm to millimeter. Theoretically, with this method, microgels with even smaller size could be obtained. But when the volume decreased, evaporation became the main problem that led to deformation of the liquid bridge. An interesting phenomenon can be observed from Figure 2a is that the fabricated dumbbell-like shaped microgels got more and more symmetrical with decreasing drop volume. For an equilibrium state of liquid bridge, a delicate balance between gravity and surface tension is achieved. A strong gravity tends to drag the liquid downward and thus pile the liquid at the bottom part. The relative importance of gravity could be characterized by the Bond number Bo = $((\rho g H^2)/\gamma)$. As mentioned above, in such a system when the scale is small, Bo $\ll$ 1 (i.e., $\rho g H^2 \ll \gamma$) and gravity is ignorable.[35,36] From the results, we can ignore the effect of gravity only when the volume is less than 0.1 μL. In most cases of this study, however, the gravity term is still retained.

To study the influence of hydrophobicity of the surfaces on the shape, we used multiple kinds of surfaces. The volume of the hydrogel precursor was fixed at 0.5 μL, and the distance between the two surfaces was fixed at 830 μm. Different kinds of surfaces mentioned above were used in the experiment, and different shapes of microgels have been obtained (Figure 2b). The glass will result in a smaller contact angle and a larger contact area, while the hydrophobic glass goes to larger contact angle and smaller contact area. So, when we use the same surface in both sides, the fabricated microgel with a dumbbell shape would show a significant difference. Specifically, microgels fabricated with hydrophobic glass have smaller "heads" and

DOI: 10.1021/acsami.5b00081
ACS Appl. Mater. Interfaces 2015, 7, 11134−11140

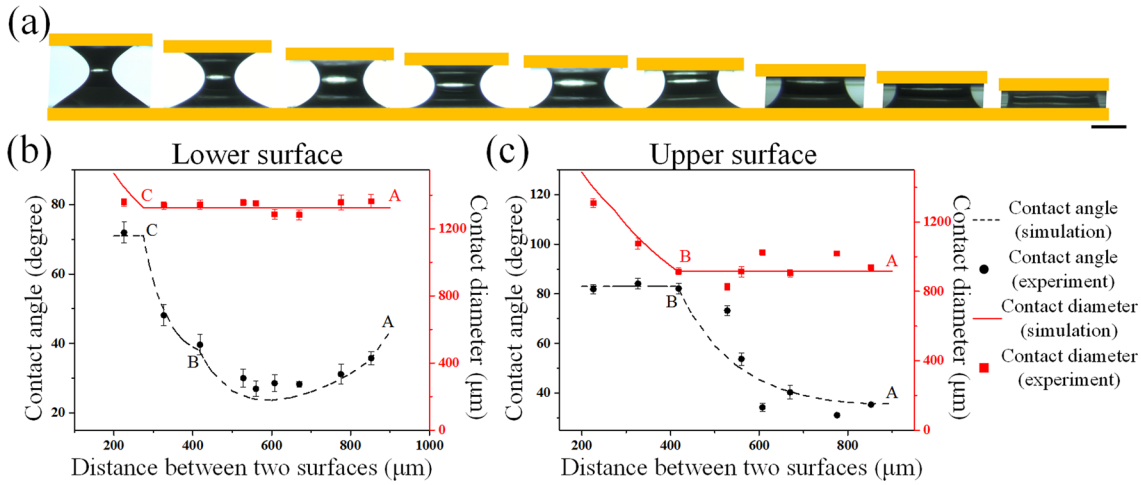

Figure 4. (a) Images of microgels with different geometries caused by controlling *H*. (b and c) Comparison between experimental and simulation results for the contact angle and contact radius of the microgels. The results shown were for PMMA surface. The liquid was gelatin, and the volume was fixed at 0.35 μL. Scale bar: 500 μm.

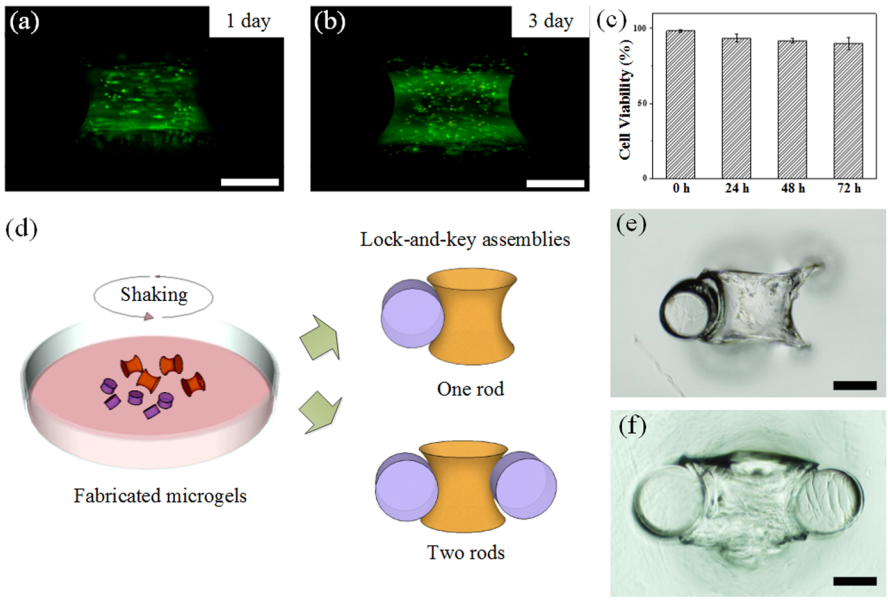

Figure 5. Fluorescent image of live/dead staining of cells in hydrogels at (a) t = 24 h and (b) t = 72 h (green represents live cells, red represents dead cells); (c) statistical results of cell viability; (d) schematic of directed assembly of dumbbell-like and rod-shaped microgels; (e and f) phase-contrast images of dumbbell-like and spherical microgel assemblies with one to two rods per dumbbell. Scale bar = 250 μm.

larger "waists"; however, when the surface was changed into glass, microgels with larger heads and smaller waists can be obtained. Consider the effect of gravity: funnel shaped microgels can be obtained with hydrophobic glass in the upper side and glass in the lower side. The results indicated that hydrophobicity of the surfaces can significantly influence the shapes of the microgels. We also achieved more complicated microstructures using surface with irregular shapes (Figure 2c). With a needle, we can get a hemispherical microgel with a small bump on the top. With a slice of PMMA, a nonrotational shaped microgel with a line as the upper surface was obtained. Meanwhile, microgels with cambered upper surface were fabricated with cambered PMMA surfaces that have a different radius of curvature.

After generating the hydrogel precursor arrays, microgel arrays with uniform shape can be easily obtained (Figure 3a–d). We have fabricated a 10 × 10 microgel array with PMMA in both sides and a 7 × 10 microgel array with hydrophobic glass on the upper side and glass on the lower side, indicating the high-throughput capability of our method. With PAAM the fabricated microgels were dumbbell shaped (Figure 3a,b), while with hydrophobic glass and glass, the fabricated microgels were funnel shaped (Figure 3c,d). From the magnified images (Figure 3b,d), we can see that the fabricated microgels were highly uniform, stable, and robust. To test the compatibility of our method with different types of hydrogels, we used temprature-sensitive hydrogel (gelatin), photosensitive hydrogel (PEG), and chemical cross-linked hydrogel (PAAm; Figure 3e–g). The results indicated that all these hydrogels can be fabricated with tailored microstructures using such an approach. Such a simple and facile fabrication method also holds potential for mimicking 3D cellular mechanical microenvironment in vitro by stretching/compressing liquid bridge microgels between two solid surfaces.

DOI: 10.1021/acsami.5b00081
ACS Appl. Mater. Interfaces 2015, 7, 11134–11140

To demonstrate that the shape of the microgels can be predict by the developed mathematical model, we made a comparison between the experimental data and the simulation results (Figure 4). The experimental data was obtained in PMMA surface with 0.35 μL of gelatin, and Figure 4a shows images of the fabricated microgels with different heights. The hydrogel precursor liquid bridge was first stretched to the maximum extent and subsequently compressed to the intended positions to be cross-linked, and the error bar represented three results. To reduce the influence of evaporation during the synthesis and measurement process, an air humidifier was used, and because the gelatin solidifies at 16 °C within 30 s, the contact angle did not change significantly (Figure S1, Supporting Information). It can be observed that the experiment results (symbols) well match the simulation (lines). At the beginning, when the liquid bridge was stretched to the maximum extent (point A), the contact angle (CA) was between its advancing contact angle (θ_a) and receding contact angle (θ_r) on both surfaces, which results in the contact diameter stay the same at first compression stage. With decreasing H, the CA on acceptor surface first reached θ_a (point B), then the CA on donor surface reached θ_a (point C). After CA reached θ_a, it remained constant; meanwhile, the contact diameter began to expand until H reached the minimum. An intriguing phenomenon can be observed that the CA on the acceptor surface increased with the H decreasing, which was easy to accept, while the CA on the donor surface decreased at the initial compression stage. The intuition, however, is that the CA should also increase when the liquid bridge is compressed, which was opposite to the experimental results and numerical prediction. The possible reason is that, for an axisymmetric liquid bridge, the curvature depends on two terms, as shown in eq 2, and there is a trade-off between the effects of these two terms, that is, when lowering the top plate, the first term tended to increase the CA, while the second one acted against it. Combining these two effects, the contact angle decreased first and then increased as compressing. Specifically, there exists a point (point B) between points A and C in the compression stage, where the CA on the acceptor reached its θ_a and caused a kink in the curve. Although the same surface was used in the experiment, the CA and contact diameter were different on acceptor and donor surfaces when H was fixed. This asymmetry was mainly caused by gravity.

To explore the use of the microgels fabricated here for biomedical applications, we encapsulated 3T3 cells within Gel-MA microgels and confirmed the viability of cells by using calcein AM-ethidium homodimer (Figure 5a–c). The results showed that, a high fraction (>98%) of cells were viable after cell encapsulation, and the cell viability remained high (~89%) after culture for 72 h. These results indicated that such fabrication method holds great potential for generating cell-laden building blocks and used for bottom-up tissue engineering approach. To demonstrate the utility of such strategy for generating complex and directed structures, we assembled the microgels we fabricated by using a simple two-phase assembly process. Specifically, we prepared some rod-shaped microgels using designed photomask and assembled them with the dumbbell-like microgels described above as "lock-and-key" assemblies (Figure 5d). The driving force of this kind of assembly process is the minimization of the contact area of the two-phase system. In the presence of water and oil, they tend to segregate from each other. However, with the microgels in the water phase, water and oil will finally reach an equilibrium state, which causes the solvent-exposed area to be minimized, and thus, the interaction free energy can reach its minimum. We successfully assembled lock-and-key structure and achieved ≈12% lock-and-key assemblies by using the current assembly approach without any optimization steps (Figure 5e,f). One or two rod-shaped microgels can be assembled to a dumbbell-like microgel, which indicates that such a fabrication method holds potential for constructing complex tissue constructs for tissue regeneration applications. Such simple directed assembly of liquid bridge microgels provides a powerful and highly scalable strategy to the formation of further 3D tissue constructs by the directed assembly of microengineered units. What we present above is just an example to demonstrate that the microgels fabricated with described method can be potentially used in real applications. With further decoration, more complex assembly can be achieved. For example, the microgels can be assembled by magnetic field after adding magnetic nanoparticles into the microgel;[7] with the host/guest groups, supramolecular assembly can be easily realized to overcome undesired surface and size effects;[9,10] the microengineered units can be assembled into prescribed structures with the sequence-specific "DNA glues".[41]

4. CONCLUSIONS

Here, we report a novel and facile method to fabricate microgels with tailored microstructures based on the liquid bridge phenomenon. By controlling the distance between the two substrates, the shape of the substrates, and the wetting behavior of liquid on the substrates, we can easily prepare different shapes of microgels (e.g., dumbbell-like, funnel-like and barrel-like) with accurate control. This new method draws no limitation to materials, and all kinds of hydrogels, such as temperature-sensitive, photosensitive and chemical-cross-linked hydrogels, can be put to use. Moreover, this method only requires devices that can be easily accessible to every lab. We also explored biological applications of the fabricated microgels. We encapsulated cells in the microgels and assembled the dumbbell-like microgel with rod-shaped microgel, which shows the great potential of the prepared microgels in tissue engineering.

■ ASSOCIATED CONTENT

Supporting Information

Contact angle of the precursor and the microgel. This material is available free of charge via the Internet at http://pubs.acs.org.

■ AUTHOR INFORMATION

Corresponding Author

*fengxu@mail.xjtu.edu.cn.

Author Contributions

§These authors contributed equally.

Notes

The authors declare no competing financial interest.

■ ACKNOWLEDGMENTS

This work was financially supported by the National Natural Science Foundation of China (11372243) and the Major International Joint Research Program of China (11120101002). F.X. was also partially supported by the China Young 1000-Talent Program and Program for New Century Excellent Talents in University (NCET-12-0437).

DOI: 10.1021/acsami.5b00081
ACS Appl. Mater. Interfaces 2015, 7, 11134–11140

REFERENCES

(1) Sivakumaran, D.; Maitland, D.; Hoare, T. Injectable Microgel-Hydrogel Composites for Prolonged Small-Molecule Drug Delivery. *Biomacromolecules* **2011**, *12*, 4112−4120.

(2) Du, Y.; Lo, E.; Ali, S.; Khademhosseini, A. Directed Assembly of Cell-Laden Microgels for Fabrication of 3D Tissue Constructs. *Proc. Natl. Acad. Sci. U.S.A.* **2008**, *105*, 9522−9527.

(3) Shibata, H.; Heo, Y. J.; Okitsu, T.; Matsunaga, Y.; Kawanishi, T.; Takeuchi, S. Injectable Hydrogel Microbeads for Fluorescence-Based in Vivo Continuous Glucose Monitoring. *Proc. Natl. Acad. Sci. U.S.A.* **2010**, *107*, 17894−17898.

(4) Mitragotri, S.; Lahann, J. Physical Approaches to Biomaterial Design. *Nat. Mater.* **2009**, *8*, 15−23.

(5) Liu, N.; Liang, W.; Liu, L.; Wang, Y.; Mai, J. D.; Lee, G.-B.; Li, W. J. Extracellular-Controlled Breast Cancer Cell Formation and Growth Using Non-UV Patterned Hydrogels via Optically-Induced Electrokinetics. *Lab Chip* **2014**, *14*, 1367−1376.

(6) Eydelnant, I. A.; Li, B. B.; Wheeler, A. R. Microgels On-Demand. *Nat. Commun.* **2014**, *5*, 3355.

(7) Xu, F.; Wu, C.-A.M.; Rengarajan, V.; Finley, T. D.; Keles, H. O.; Sung, Y.; Li, B.; Gurkan, U. A.; Demirci, U. Three-Dimensional Magnetic Assembly of Microscale Hydrogels. *Adv. Mater.* **2011**, *23*, 4254−4260.

(8) Xu, F.; Finley, T. D.; Turkaydin, M.; Sung, Y.; Gurkan, U. A.; Yavuz, A. S.; Guldiken, R. O.; Demirci, U. The Assembly of Cell-Encapsulating Microscale Hydrogels Using Acoustic Waves. *Biomaterials* **2011**, *32*, 7847−7855.

(9) Cheng, M.; Shi, F.; Li, J.; Lin, Z.; Jiang, C.; Xiao, M.; Zhang, L.; Yang, W.; Nishi, T. Macroscopic Supramolecular Assembly of Rigid Building Blocks Through a Flexible Spacing Coating. *Adv. Mater.* **2014**, *26*, 3009−3013.

(10) Cheng, M.; Liu, Q.; Xian, Y.; Shi, F. Programmable Macroscopic Supramolecular Assembly through Combined Molecular Recognition and Magnetic Field-Assisted Localization. *ACS Appl. Mater. Interfaces* **2014**, *6*, 7572−7578.

(11) Muro, S.; Garnacho, C.; Champion, J. A.; Leferovich, J.; Gajewski, C.; Schuchman, E. H.; Mitragotri, S.; Muzykantov, V. R. Control of Endothelial Targeting and Intracellular Delivery of Therapeutic Enzymes by Modulating the Size and Shape of ICAM-1-Targeted Carriers. *Mol. Ther.* **2008**, *16*, 1450−1458.

(12) Lee, K. J.; Yoon, J.; Lahann, J. Recent Advances with Anisotropic Particles. *Curr. Opin. Colloid Interface Sci.* **2011**, *16*, 195−202.

(13) Rolland, J. P.; Maynor, B. W.; Euliss, L. E.; Exner, A. E.; Denison, G. M.; DeSimone, J. M. Direct Fabrication and Harvesting of Monodisperse, Shape-Specific Nanobiomaterials. *J. Am. Chem. Soc.* **2005**, *127*, 10096−10100.

(14) Bian, W.; Liau, B.; Badie, N.; Bursac, N. Mesoscopic Hydrogel Molding to Control the 3D Geometry of Bioartificial Muscle Tissues. *Nat. Protoc.* **2009**, *4*, 1522−1534.

(15) Beebe, D. J.; Moore, J. S.; Bauer, J. M.; Yu, Q.; Liu, R. H.; Devadoss, C.; Jo, B. H. Functional Hydrogel Structures for Autonomous Flow Control Inside Microfluidic Channels. *Nature* **2000**, *404*, 588−590.

(16) Ma, S.; Thiele, J.; Liu, X.; Bai, Y.; Abell, C.; Huck, W. T. Fabrication of Microgel Particles with Complex Shape via Selective Polymerization of Aqueous Two-Phase Systems. *Small* **2012**, *8*, 2356−2360.

(17) Hoffmann, J. C.; West, J. L. Three-Dimensional Photolithographic Patterning of Multiple Bioactive Ligands in Poly(ethylene glycol) Hydrogels. *Soft Matter* **2010**, *6*, 5056−5063.

(18) Qin, D.; Xia, Y.; Whitesides, G. M. Soft Lithography for Micro and Nanoscale Patterning. *Nat. Protoc.* **2010**, *5*, 491−502.

(19) Champion, J. A.; Katare, Y. K.; Mitragotri, S. Making Polymeric Micro and Nanoparticles of Complex Shapes. *Proc. Natl. Acad. Sci. U.S.A.* **2007**, *104*, 11901−11904.

(20) Lee, J.; Bisso, P. W.; Srinivas, R. L.; Kim, J. J.; Swiston, A. J.; Doyle, P. S. Universal Process-Inert Encoding Architecture for Polymer Microparticles. *Nat. Mater.* **2014**, *13*, 524−529.

(21) Pregibon, D. C.; Toner, M.; Doyle, P. S. Multifunctional Encoded Particles for High-Throughput Biomolecule Analysis. *Science* **2007**, *315*, 1393−1396.

(22) Hwang, D. K.; Dendukuri, D.; Doyle, P. S. Microfluidic-Based Synthesis of Non-Spherical Magnetic Hydrogel Microparticles. *Lab Chip* **2008**, *8*, 1640−1647.

(23) Dendukuri, D.; Pregibon, D. C.; Collins, J.; Hatton, T. A.; Doyle, P. S. Continuous-Flow Lithography for High-Throughput Microparticle Synthesis. *Nat. Mater.* **2006**, *5*, 365−369.

(24) Park, S.; Kim, D.; Ko, S. Y.; Park, J.-O.; Akella, S.; Xu, B.; Zhang, Y.; Fraden, S. Controlling Uniformity of Photopolymerized Microscopic Hydrogels. *Lab Chip* **2014**, *14*, 1551−1563.

(25) Kao, Y. H.; Chi, M. H.; Tsai, C. C.; Chen, J. T. Nanopressing: Toward Tailored Polymer Microstructures and Nanostructures. *Macromol. Rapid Commun.* **2014**, *35*, 84−90.

(26) Gorb, S. N. The Design of the Fly Adhesive Pad: Distal Tenent Setae are Adapted to the Delivery of an Adhesive Secretion. *Proc. R. Soc. B* **1998**, *265*, 747−752.

(27) Eisner, T.; Aneshansley, D. J. Defense by Foot Adhesion in a Beetle (*Hemisphaerota cyanea*). *Proc. Natl. Acad. Sci. U.S.A.* **2000**, *97*, 6568−6573.

(28) Dixon, A.; Croghan, P.; Gowing, R. The Mechanism by which Aphids Adhere to Smooth Surfaces. *J. Exp. Biol.* **1990**, *152*, 243−253.

(29) Federle, W.; Riehle, M.; Curtis, A. S.; Full, R. J. An Integrative Study of Insect Adhesion: Mechanics and Wet Adhesion of Pretarsal Pads in Ants. *Integr. Comp. Biol.* **2002**, *42*, 1100−1106.

(30) Qian, B.; Breuer, K. S. The Motion, Stability, and Breakup of a Stretching Liquid Bridge with a Receding Contact Line. *J. Fluid Mech.* **2011**, *666*, 554−572.

(31) Darhuber, A. A.; Troian, S. M.; Wagner, S. Physical Mechanisms Governing Pattern Fidelity in Microscale Offset Printing. *J. Appl. Phys.* **2001**, *90*, 3602−3609.

(32) Kang, H. W.; Sung, H. J.; Lee, T.-M.; Kim, D.-S.; Kim, C.-J. Liquid Transfer Between Two Separating Plates for Micro-Gravure-Offset Printing. *J. Micromech. Microeng.* **2009**, *19*, 015025.

(33) Bonn, D.; Eggers, J.; Indekeu, J.; Meunier, J.; Rolley, E. Wetting and Spreading. *Rev. Mod. Phys.* **2009**, *81*, 739−805.

(34) Moon, D.; Im, D. J.; Lee, S.; Kang, I. S. A Novel Approach for Drop-on-Demand and Particle Encapsulation Based on Liquid Bridge Breakup. *Exp. Therm. Fluid Sci.* **2014**, *53*, 251−258.

(35) Chen, H.; Amirfazli, A.; Tang, T. Modeling Liquid Bridge Between Surfaces with Contact Angle Hysteresis. *Langmuir* **2013**, *29*, 3310−3319.

(36) Su, Y.; Ji, B.; Huang, Y.; Hwang, K. Effects of Contact Shape on Biological Wet Adhesion. *J. Mater. Sci.* **2007**, *42*, 8885−8893.

(37) Ajaev, V. S.; Homsy, G. Modeling Shapes and Dynamics of Confined Bubbles. *Annu. Rev. Fluid Mech.* **2006**, *38*, 277−307.

(38) Reddy, J. N. *An Introduction to the Finite Element Method*; McGraw-Hill: New York, 1993.

(39) Yang, Q.; Li, B. Q.; Ding, Y. A Numerical Study of Nanoscale Electrohydrodynamic Patterning in a Liquid Film. *Soft Matter* **2013**, *9*, 3412−3423.

(40) Xu, F.; Inci, F.; Mullick, O.; Gurkan, U. A.; Sung, Y.; Kavaz, D.; Li, B.; Denkbas, E. B.; Demirci, U. Release of Magnetic Nanoparticles from Cell-Encapsulating Biodegradable Nanobiomaterials. *ACS Nano* **2012**, *6*, 6640−6649.

(41) Qi, H.; Ghodousi, M.; Du, Y.; Grun, C.; Bae, H.; Yin, P.; Khademhosseini, A. DNA-Directed Self-Assembly of Shape-Controlled Hydrogels. *Nat. Commun.* **2013**, *4*, 2275.

DOI: 10.1021/acsami.5b00081
ACS Appl. Mater. Interfaces 2015, 7, 11134−11140